The Effect of Parapets on the Performance of Unglazed Solar Collectors

Delight M. Sedzro [1], T. N. Anderson[1] and Roy Nates [1]
[1]*Auckland University of Technology, Auckland, New Zealand*
Morkporkpor.sedzro@aut.ac.nz, timothy.anderson@aut.ac.nz, roy.nates@aut.ac.nz

Abstract: Roof-mounted unglazed solar collectors are one of the most promising low-cost renewable energy technologies. However, their application is limited due to wind-induced heat loss which reduces their performance. That said, the wind flow over roof surfaces, where solar collectors are typically mounted, can be affected by a host of parameters related to the surrounding terrain and building topology. Perimetric parapets have shown an ability to reduce wind loads on roofs, particularly in low-rise buildings, and it is conceivable that this may also benefit solar collectors. Studies related to the effect of parapets on roof-mounted solar technologies have however been limited to wind loads on roof-top equipment or structural support systems, rather than on the heat loss. In this study, the performance of an unglazed solar collector mounted on a low-rise building with perimetric parapets was examined through wind tunnel experiments and computational fluid dynamics (CFD) simulations. The average pressure coefficients determined from the wind tunnel measurements were used to validate steady-state 3D Reynolds Averaged Navier-Stokes simulations. Subsequently, simulations were carried out for different wind velocities and directions with variations in parapet height. When normalised with Reynold's and Nusselt numbers, the results showed the quantitative effect of these parameters. It is shown how sensitive the thermal performance of the collector is to parapet height, wind velocity and collector mounting location.

Keywords: Solar Collector, CFD, Parapets. **Keywords:** Solar Collector, CFD, Parapets

1. Introduction

Parapets can be described as outwardly designed architectural features, that take the form of solid or segmented attachments to the roof of a building, or, an extension from it. Often, the intent of parapets or similar building features, are ornamental, although most function as structures which visually obscure, from the ground or other levels, the lateral view of building services equipment. Its influence on local pressure coefficients and roof wind loads have been the focus of several numerical and experimental studies. For buildings with flat roofs, the effect of parapets on wind induced pressure coefficients under uniform and turbulent flow conditions has been documented, see (Baskaran and Stathopoulos, 1988; Kopp et al., 2005b; Lythe and Surry, 1983).

Imaginable Futures: Design Thinking, and the Scientific Method. 54th International Conference of the Architectural Science Association 2020, Ali Ghaffarianhoseini, et al (eds), pp. 1095–1104.

Nonetheless, as the integration of various renewable energy technologies to buildings continues to draw significant interest, the effect of parapets on roof mounted technologies such as solar have received marked attention. These have however tended to focus on how wind loads affect solar support structures (Browne et al., 2013; Cao et al., 2013; Kopp et al., 2012; Mier-Torrecilla et al., 2014). This is particularly true in low rise buildings where the flow motion is characterized by flow separations, attachments, and the creation of vortices. In fact several studies have demonstrated that perimetric parapets can mitigate wind loads by influencing wind velocity at varying heights and configurations, (Cao et al., 2013; Lythe and Surry, 1983; Stathopoulos et al., 1999; Stathopoulos and Baskaran, 1987).

That said, very few studies have however explored the impact of parapets on the performance of solar technologies, which is interesting given that their thermal performance is influenced by the local wind velocity. In particular, unglazed solar thermal collectors have been limited to low temperature application due to the high heat losses induced by convective heat transfer to the surroundings. In terms of cost however, Burch et al., (2005) argue that the cost saving associated with unglazed collectors is higher compared to other types of solar collectors.

Given that solar thermal collectors installed on the roof top of buildings have become popular in recent times, there is the need to critically investigate the relation between some roof top features such as parapets and how they affect convective heat loss. Furthermore, with the current focus on ensuring that solar technologies aesthetically appeal or appear as part of the facades architectural concept (Chemisana, 2011), the location of roof mounted collectors relative to parapets remain of great interest. This then raises questions as to whether passive wind breaks, such as parapets, could be used to reduce the heat loss experienced by these collectors. Or, in the case of photovoltaic modules, could these windbreaks alternatively be used to increase the cooling of these panels to improve their efficiency.

2. Method

To determine the relationship between parapets and the heat transfer from unglazed solar collector, it was decided to undertake a simulation study using a commercial 3-D steady-state computational fluid dynamics (CFD) solver (ANSYS Fluent), to be followed by an experimental validation of the method.

2.1. Numerical modelling

In undertaking the CFD analysis, three model geometries of a standalone solar collector mounted on a flat roof building were modelled; without parapets, with a low perimetric parapet height of 0.03m and with a high perimetric parapet of height 0.06m. These were chosen to represent low ($h/(H+h) \leq 0.17$) and high ($h/(H+h) \geq 0.23$) parapets (where h is the parapet height and H is the building height) as documented by Kopp et al., (2005a) and were generated using the ANSYS design tool SpaceClaim.

To capture the flow field, a computational domain was developed as detailed in best practice guidelines by Franke et al., (2007). Accordingly, the domain allowed 5H between the inflow boundary and the lateral sides of the buildings (where H is the vertical height from the trailing edge of the collector to the base of the building), and was extended 15H downstream of the building to capture all other affected parameters at wind incidence of 0^o and 45^o, see Figure 1.

Higher resolution meshes were generated around the collector, parapet, and roof top. Regions away from the buildings were however of coarse mesh to improve computational speed. Overall, the whole computational boundary domain was discretized using hexahedral meshes after which they were converted to polyhedral. This was done to reduce cell counts and convergence time. Skewness was

nonetheless maintained below 0.80. Two bodies of influence were used around the building and collector to refine the mesh around these regions. Six inflation layers with first cell height of 0.1mm was used to capture the boundary layer on the collector surface. The first cell height was varied to achieve a y+ value of less than 1 on the collector surface. A mesh sensitivity analysis was also undertaken to ensure that the computational method is independent of number of elements.

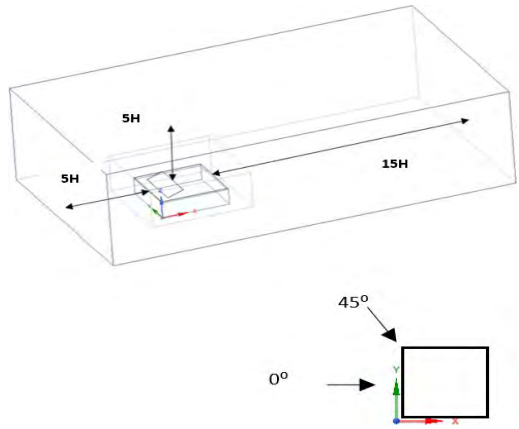

Figure 1: Computational domain

For the inlet boundary condition in each case, a uniform constant inflow velocity (u) 10 m/s was adopted as the inlet boundary condition and defined as velocity inlet. The bottom boundary condition was set as a non-slip wall, while the top boundary conditions was specified as symmetry. The outlet boundary condition was specified as pressure outlet. For the $kk-\varepsilon\varepsilon$ turbulence model, realizable was used for the closure of the transport equation. The SIMPLE algorithm scheme was used as the pressure velocity coupling. Pressure interpolation in second order and second-order discretization schemes were specified for both the convection and the viscous terms of the governing equations. The solution was initialized by the values of the inlet boundary conditions. The chosen convergence criterion was specified so that the residuals decreased to 10^{-6} for all the equations. To ascertain the heat transfer, the collector was assumed as an isothermal plate at a constant temperature of 333K with an ambient temperature of 303K throughout the domain.

2.1. Experimental method

In line with validating the numerical simulation for this study, experimental studies were conducted in the Atmospheric Boundary Layer (ABL) Wind Tunnel at the University of Auckland. The test section of the wind tunnel is 20 m long, 2.5 m high, and 3.6 m wide. The test model made of polymethyl methacrylate sheet (see Figure 2), was constructed at a length scale of 1:20 to accurately model the rooftop perimetric parapets and to measure the wind pressures on the requisite surfaces. The model dimensions were 0.8m (D) × 0.8 m (B) × 0.2m (H) representing a height to breadth ratio of 1:4 and

breadth to depth ratio of 1:1. A flat plate of thickness 0.003m, and dimension 0.4m (L) × 0.2m (B) was mounted on the flat roof of the buildings at a tilt angle of 20°. Here, the flat plate was set at different locations of 0.2m, 0.4 and 0.6m on the roof. Two parapet heights 0.03m, 0.06m were considered.

Overall, 100 pressure taps were uniformly distributed across the model: 5 on the surface of each parapet, 50 on the roof and 30 on the upper surface of the collector (flat plate). The wind directions were varied from 0° to 90° in the wind tunnel test. Two approaching flow characteristics were considered, a uniform and an open flat terrain with a ground roughness terrain category 2 based on AS/NZS1170.2 (2011). In the current study however, wind direction of 0°, collector location of 0.2m, parapet height 0.03m and a free stream velocity of 10m/s are reported for the validation of the numerical model.

Figure 2: Experimental set up with model and collector in wind tunnel

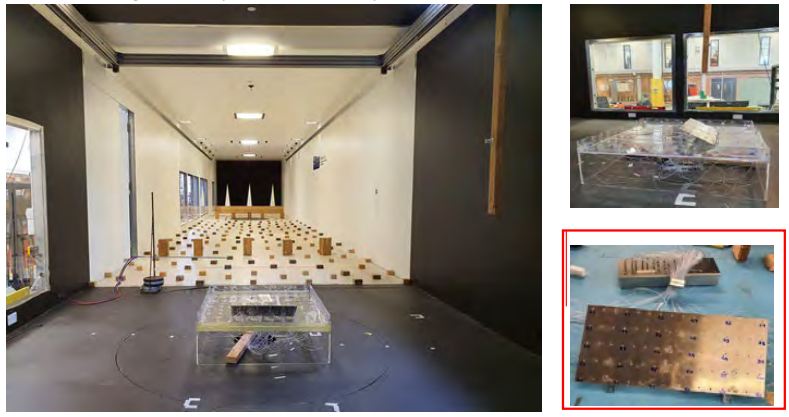

2.3. Model validation

To validate the numerical results, the experimental results were compared in terms of flow visualization and the pressure coefficient distribution on the surface of the collector, parapet, and roof. The wind pressure coefficient at specific taps, C_{pi}, were determined by Equation 1. Where P_{∞} is the static pressure at infinity, ρ is the air density, U_{ref} is the mean wind velocity and $P_{i(t)}$ is the pressure measured at the tap. The pressure coefficient at the same location on the experimental model was compared to that on the simulated model, as shown in Figure 3. Similarly, the flow around the collector at 0^{o} for both methods were also compared as shown Figure 4. Both methods of validation showed a good agreement between the experimental and computational data.

$$C_{pi} = \frac{P_{i\,(t)} - P_{\infty}}{0.5\,\rho\,U_{ref}{}^{2}} \tag{1}$$

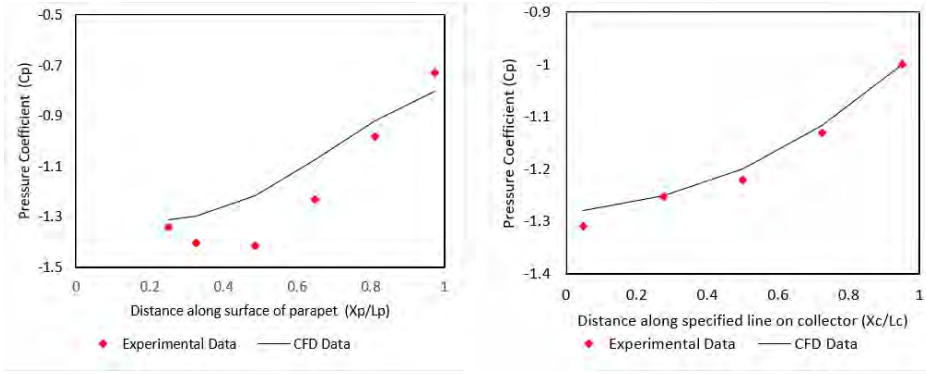

Figure 3: Comparison of experimental and numerical data for low parapet (h/(H+h) ≤ 0.17) at 5m/s. Where Xc is the position long surface of collector, Lc is the length of collector, Xp is the position along the face of the parapet and Lp is the length of parapet.

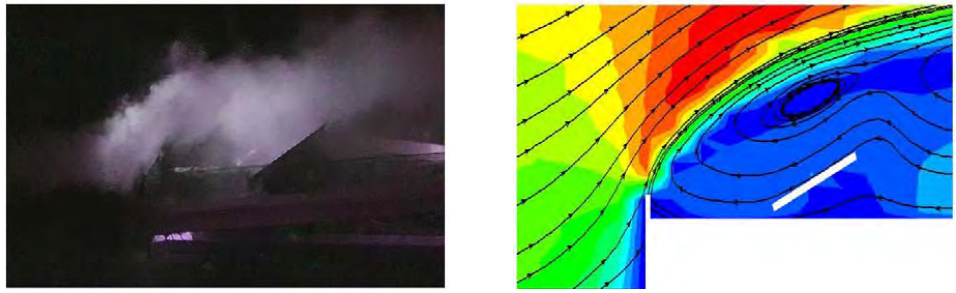

(a) (b)

Figure 4: (a) Photograph of flow visualization in wind tunnel test (b) Flow visualization with contours and streamline in vertical plane of CFD for 0˚ wind incidence and collector location of 0.2m

3. Results and discussion

Having validated the modelling method, it was decided to examine the flow behaviour and heat loss for a broader range of conditions than could be examined experimentally. Figure 5 shows the flow topologies of the 3D model on the mid isoplane (y=0.4). By examining the influence of the parapet height on the flow around the collector at 5m/s and wind incidence 0˚, it is observed that the flow impinges directly on the surface of the collector. This is influenced by the flow separation at the edge of the roof. Without the parapets (Figure 5 a), a recirculation bubble is created on the windward side of the collector along with higher wind velocity as shown in the contours. Now, when a lower parapet is

installed as shown in figure 5 b, the recirculation bubble extends although with reduced velocity as depicted in the contours. As expected, an increase in the perimetric parapet as shown in figure 5c, shows a reduction in the velocity near the surface of the collector. Again, a larger recirculation bubble is formed upstream of the collector which extends towards the trailing edge of the collector.

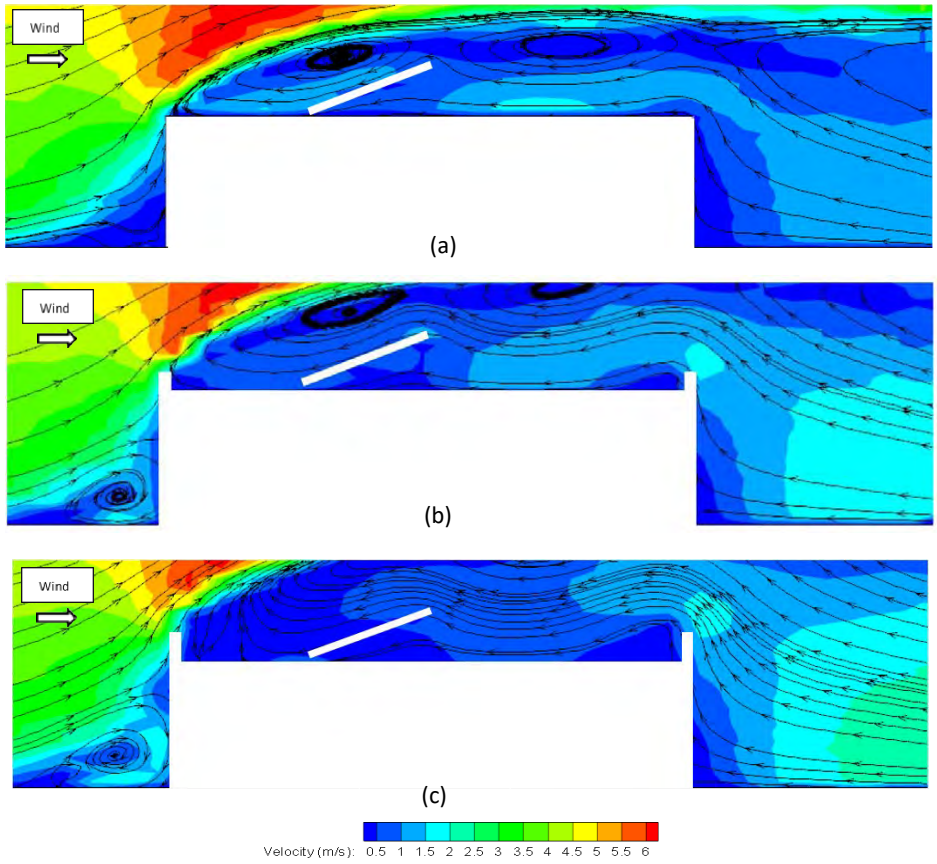

Figure 5: Contours of mean velocity magnitude (5m/s) with streamlines at 0˚ incidence and 0.6m collector location for (a) no parapet (b) low parapet (c) high parapet

When the collector is moved 0.6m away from the edge of the collector (at mid isoplane y=0.4m), a different observation is made. As shown in Figure 6, larger recirculation bubbles are created in all cases. The position of the recirculation bubbles however varies with change in the height of the parapet. For flat roof without parapet, the oncoming flow impinges on the surface of the collector forming a smaller recirculation bubble (see Figure 6a). The velocity contours show the wind velocity is high in this case.

The reversed flow is also lower compared to that of the higher parapet. As the height of the parapet increases, the bubble upstream of the collector expands, separating at the trailing edge of the collector. Higher wind velocity however exists on the surface of the collector at the higher parapet (Figure 6c) compared to velocities at lower parapet (Figure 6b).

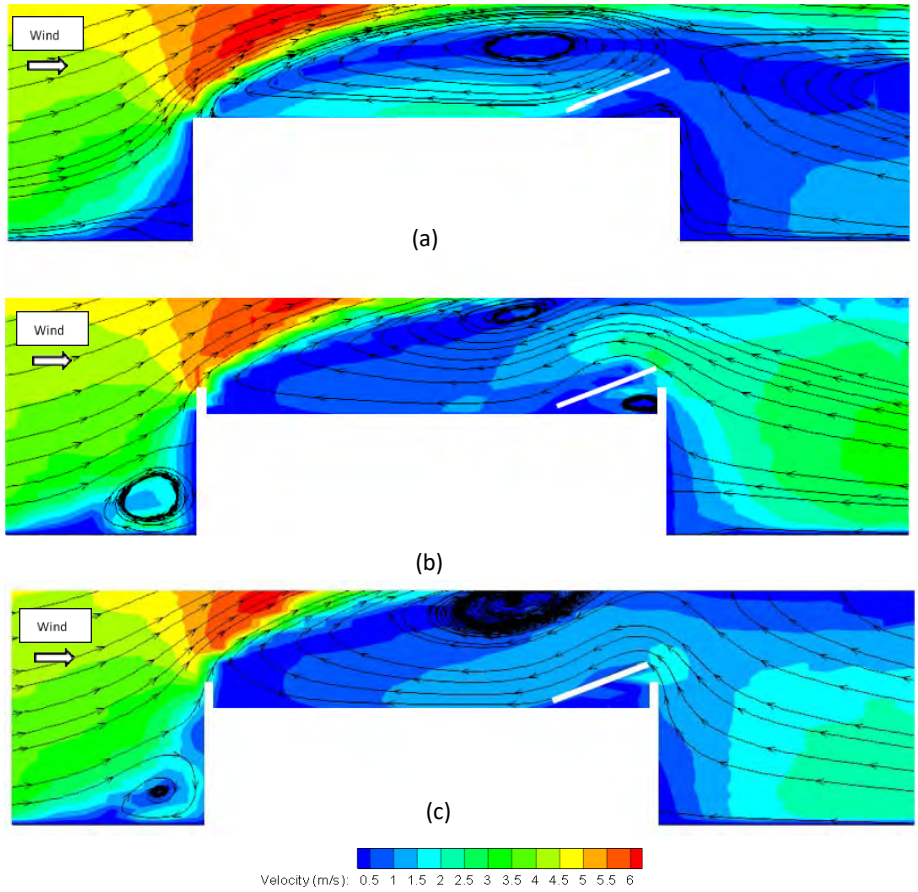

Figure 6: Contours of mean velocity magnitude (5m/s) with streamlines at 0˚ incidence and 0.6m collector location for (a) no parapet (b) low parapet (c) high parapet

Now, the flow fields of the 3D model on the isoplane (x=2.3) at 45˚ wind incidence is examined. Figure 7 displays the velocity magnitude on the roof with higher perimetric parapets, in plan view. At the 0.2m location, a higher wind velocity is observed on both the leeward and windward side of the

collector. This is due to the closeness of the collector to the parapet and leading edge of the building where the flow separation is predominant, see Figure 7 (a). When the collector is moved further away at 0.4m, higher wind velocities are observed on windward side of the collector while lower velocities are seen at the leeward side of the collector.

Evidently, the flow separation at the leading edge of the building to the 45˚ wind incidence impinges more on the surface of the collector, leading to higher velocities at its sideward edges (See Figure 7b). The above observation is even marked at the collector location of 0.6m where higher velocities (5m/s) are seen around a greater part of the collector.

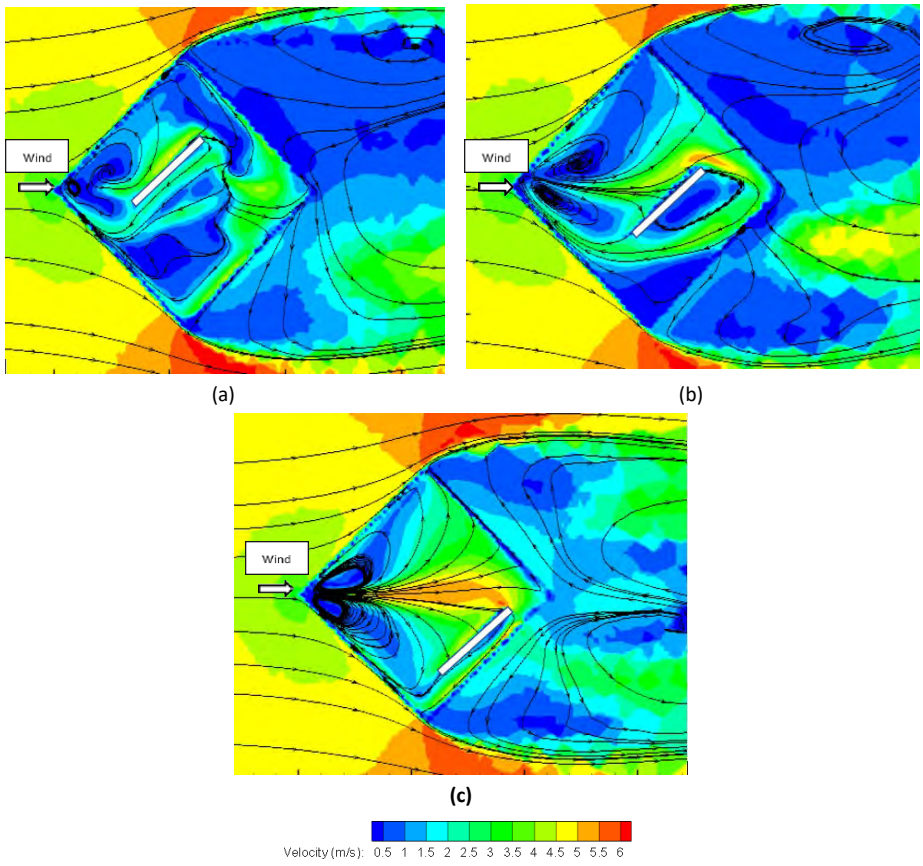

Figure 7: Contours of mean velocity magnitude (5m/s) at 45˚ incidence at high parapet for (a) 0.2 m collector location (b) 0.4 collector location (c) 0.6 collector location

Finally, given that the topology of the flow and wind velocity around the collector is decisive in the amount of convective heat loss, the effect of parapets on heat loss is analysed. To do this, a generalized

relation of aspect ratio (L/h) is determined, where L is the length of the cavity of the roof and h, the height of the parapet. For the case of no parapet, the aspect ratio is defined at infinity (∞), where h is assumed in this case to be some arbitrary number. The wind velocity is also varied between 2m/s to 10m/s, chosen based on studies such as Soltau, (1992). As shown in Figure 8, the average Nusselt number Nu_{avg} decreases at a lower aspect ratio for the same Reynolds numbers (Re). This is primarily due to vortices created behind the parapets, especially in the case of higher parapets, consistent a similar observation made by Mesalhy et al., (2010) for flows in shallow cavities. When the Reynolds number, is increased, it is observed that Nu_{avg} increases accordingly. Nu_{avg} is however lower at infinity where no parametric parapets are installed.

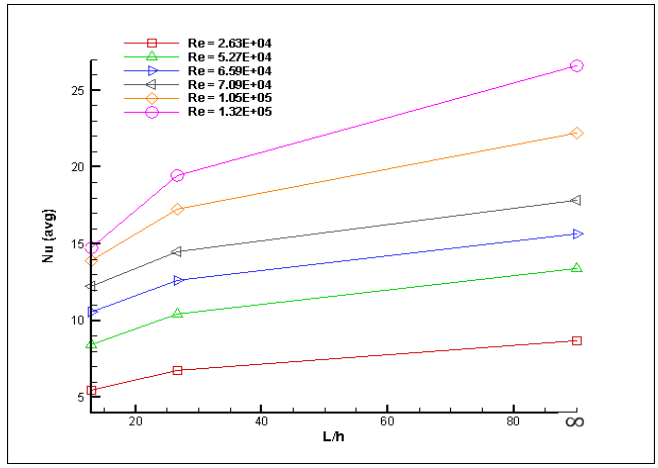

Figure 8: Effect of changing cavity aspect ratio on average Nusselt number at 0.2m collector location

4. Conclusions

Analysis of the data reported above suggest a promising benefit of parapets to roof mounted solar technologies, particularly unglazed solar thermal collectors. The most obvious fact is that parapets can minimise the local velocities around collectors, leading to a reduction in convective heat loss. For collector placed on roofs with higher parapets, this could be advantageous albeit the effect of shading cannot be overlooked. The data show Nu_{avg} is sensitive to aspect ratio (L/h) and Reynolds number. Notwithstanding this observation, the data presented show significant changes in flow topology depending on the location of the collector away from the parapet. The further the collector is moved away from the parapet, the lesser its likelihood to minimise the wind velocity. What this suggests is that, collectors placed very far away from the parapet are likely to experience the same velocities with or without the parapets in place. Now, collector inclination angle and wind incidence angle are significant in evaluating the performance of solar thermal collectors, thus there is a significant scope in estimating the sensitivity of Nu_{avg} to these factors at varying parapet height and collector location.

Acknowledgements

The authors would like to thank Professor Richard Flay and Dr Yin Fai Li of the University of Auckland for providing access to the wind tunnel.

References

Aly, A. M. (2016) 'On the evaluation of wind loads on solar panels: The scale issue', Solar Energy. doi: 10.1016/j.solener.2016.06.018.

Baskaran, A. and Stathopoulos, T. (1988) 'Roof corner wind loads and parapet configurations', Journal of Wind Engineering and Industrial Aerodynamics. doi: 10.1016/0167-6105(88)90147-X.

Browne, M. T. L. et al. (2013) 'Wind loading on tilted roof-top solar arrays: The parapet effect', Journal of Wind Engineering and Industrial Aerodynamics. doi: 10.1016/j.jweia.2013.08.013.

Burch, J., Salasovich, J. and Hillman, T. (2005) 'An assessment of unglazed solar domestic water heaters', in Proceedings of the Solar World Congress 2005: Bringing Water to the World, Including Proceedings of 34th ASES Annual Conference and Proceedings of 30th National Passive Solar Conference.

Cao, J. et al. (2013) 'Wind loading characteristics of solar arrays mounted on flat roofs', Journal of Wind Engineering and Industrial Aerodynamics. doi: 10.1016/j.jweia.2013.08.014.

Chemisana, D. (2011) 'Building integrated concentrating photovoltaics: A review', Renewable and Sustainable Energy Reviews. doi: 10.1016/j.rser.2010.07.017.

Duffie, J. A. and Beckman, W. A. (2013) Solar Engineering of Thermal Processes: Fourth Edition, Solar Engineering of Thermal Processes: Fourth Edition. doi: 10.1002/9781118671603.

Franke, J. et al. (2007) Best practice guideline for the CFD simulation of flows in the urban environment, COST action.

Hottel, H. C. and Whillier, A. (1958) 'Evaluation of flat-plate solar-collector performance', Transactions of the Conference on Use of Solar Energy.

Huang, P., Peng, X. and Gu, M. (2017) 'Wind tunnel study on effects of various parapets on wind load of a flat-roofed low-rise building', Advances in Structural Engineering. doi: 10.1177/1369433217700425.

Jürges, W. (1924) 'Der Wärmeübergang an einer ebenen Wand Beih.', zum Gesundh.-Ing., pp. 1227–1249.

Kopp, G. A., Farquhar, S. and Morrison, M. J. (2012) 'Aerodynamic mechanisms for wind loads on tilted, roof-mounted, solar arrays', Journal of Wind Engineering and Industrial Aerodynamics. doi: 10.1016/j.jweia.2012.08.004.

Kopp, G. A., Mans, C. and Surry, D. (2005) 'Wind effects of parapets on low buildings: Part 2. Structural loads', Journal of Wind Engineering and Industrial Aerodynamics. doi: 10.1016/j.jweia.2005.08.005.

Kopp, G. A., Surry, D. and Mans, C. (2005) 'Wind effects of parapets on low buildings: Part 1. Basic aerodynamics and local loads', Journal of Wind Engineering and Industrial Aerodynamics. doi: 10.1016/j.jweia.2005.08.006.

Lythe, G. and Surry, D. (1983) 'Wind loading of flat roofs with and without parapets', Journal of Wind Engineering and Industrial Aerodynamics. doi: 10.1016/0167-6105(83)90091-0.

McAdams, W. H. (1954) Heat Transmission (third ed.),. third ed. Kogakusha, Tokyo, Japan: McGraw-Hill.

Mesalhy, O. M., Abdel Aziz, S. S. and El-Sayed, M. M. (2010) 'Flow and heat transfer over shallow cavities', International Journal of Thermal Sciences. doi: 10.1016/j.ijthermalsci.2009.09.007.

Mier-Torrecilla, M., Herrera, E. and Doblaré, M. (2014) 'Numerical calculation of wind loads over solar collectors', in Energy Procedia. doi: 10.1016/j.egypro.2014.03.018.

Soltau, H. (1992) 'Testing the thermal performance of uncovered solar collectors', Solar Energy. doi: 10.1016/0038-092X(92)90005-U.

Stathopoulos, T. and Baskaran, A. (1987) 'Wind pressures on flat roofs with parapets', Journal of Structural Engineering (United States). doi: 10.1061/(ASCE)0733-9445(1987)113:11(2166).

Stathopoulos, T., Marathe, R. and Wu, H. (1999) 'Mean wind pressures on flat roof corners affected by parapets: Field and wind tunnel studies', Engineering Structures. doi: 10.1016/S0141-0296(98)00011-X.

Stathopoulos, T. and Zhou, Y. S. (1995) 'Numerical evaluation of wind pressures on flat roofs with the k-ε model', Building and Environment. doi: 10.1016/0360-1323(94)00038-T.